Journal of Applied Polymer Science

The Design and Performance of a Vane Mixer Based on Extensional Flow for Polymer Blends

Yin Xiaochun,[1] Yu Zhongwei,[1] Zengwenbing,[2] He Guangjian,[1] Yang Zhitao,[1] Xu Baiping[3]

[1]Key Laboratory of Polymer Processing Engineering of Ministry of Education, South China University of Technology, Guangzhou 510640, China

[2]Hubei Sanjiang Space Wan Feng Technology Development Co. Ltd., Xiaogan 432000, Hubei, China

[3]Department of Chemical Engineering, Guangdong Industry Technology College, Guangzhou 510300, China

Correspondence to: Y. Zhitao (E-mail: meztyang@scut.edu.cn)

ABSTRACT: A new laboratory-scale mixing device called the "Vane Mixer" was designed, built, and tested. The vane mixer consists of three vane plasticizing and conveying unit. In comparison with the existing laboratory mixers, material flow in this vane mixer is characterized by a high contribution from extensional flow. As the mixer has mixing chamber of very simple geometry, the cleaning is very easy and the material lost is very small. The influences of mixing time and rotor speed on dispersed phase size were characterized and discussed. Morphology data on model immiscible polystyrene/high density polyethylene (PS/HDPE) blend have proved the high distributive and dispersive mixing efficiency. © 2014 Wiley Periodicals, Inc. J. Appl. Polym. Sci. **2015**, *132*, 41551.

KEYWORDS: morphology; composites; polystyrene; blends

Received 3 July 2014; accepted 22 September 2014
DOI: 10.1002/app.41551

INTRODUCTION

Blending of polymers is one of the most promising routes for producing desired materials rather than synthesizing new materials. One of the key factors in achieving desired final properties is the control of phase morphology. The type of mixer used has considerable influence on controlling the morphology. Most polymer blends and composites were manufactured in twin-screw extruders or batch mixer dominated by shear deformation. However, it is recognized that the mixing process dominated by extensional deformation has many advantages such as better dispersive and distributive mixing, reduced melt temperature, and wide adaptability.[1,2] Some researches about deformation, break up, and coalescence mechanisms of dispersed droplets under extensional flow were performed on elongational rheometers[3,4] or four-roll mill geometry,[5] which are difficult to use in an industrial mixing process. Another simple way to generate extensional flow in compounding equipment is to use convergent/divergent flow conditions. Meller et al.[6,7] used a capillary rheometer equipped with dies of different entry profiles to study the deformation and break up of dispersed droplets in molten polymer blends of different viscosities. They showed that deformation and break up of dispersed droplets is easier in extensional flow field than in shear flow field and this is particularly true for systems with high viscosity ratios. Moreover, the mixing efficiency in the converging flow zone was dependent both on the shape of the convergence and on the volume flow rate. Utracki and Luciani[8] developed an extensional field that can be used in industrial mixing process when attached to an extruder. Son[9] designed a batch mixer according to the concept of multipass rheometer[10] in which an unlimited number of convergent/divergent flows can be applied to the material to be mixed. Bouqey[11] designed a mixing device based on the geometry of Mackley's multipass rheometer. The high distributive and dispersive mixing capability of the device was analyzed by volume finite numerical simulation of the flow within the mixer. Rauwendaal[12–14] generated double extensional flow field by creating tapered slot on the wedge screw flight. The melt suffers dual extensional forces when it crosses the cuneiform flight and tapered groove. Terrisse[15] put a removable static mixing element, which was a simple cylindrical die between two opposite cylindrical chambers. This mixing element could generate convergent and divergent flows at the entrance and exit of the die, respectively.

However, the aforementioned studies were performed on the equipment in which the extensional deformation is local and fixed. Qu[16,17] invented a type of wholly novel nonscrew plasticizing processing equipment known as vane extruder. The materials were plasticized and conveyed under the action of a dynamic extensional deformation, which could remarkably shorten the thermomechanical history, reduce the energy consumption, and improve the blending performances.[18] In this

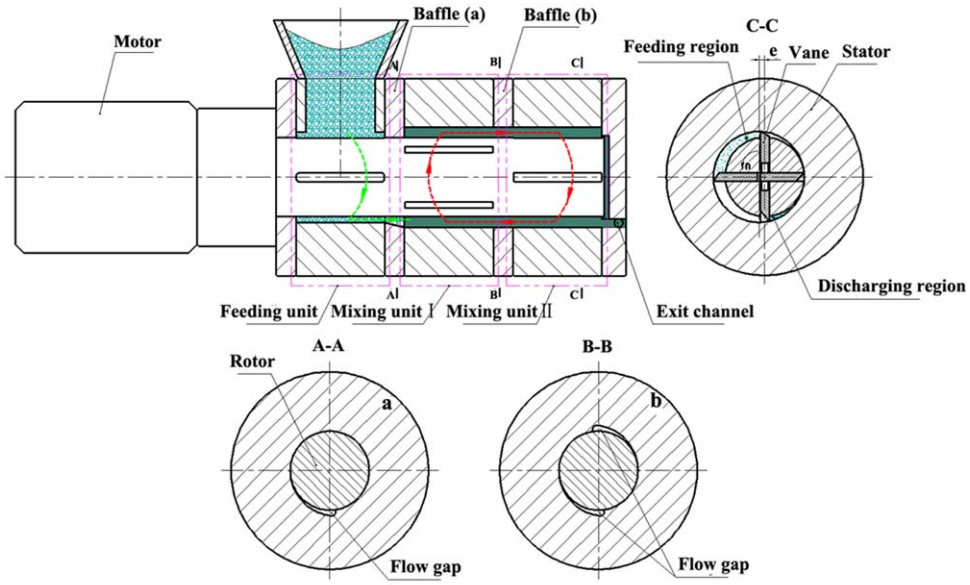

Figure 1. Schematic drawing of the vane mixer. [Color figure can be viewed in the online issue, which is available at wileyonlinelibrary.com.]

article, we describe a new mixing device based on the geometry of Qu's vane extruder. The design was significantly modified as to generate periodically changed convergent and divergent flow during the mixing procedure. The efficiency of the new mixer was tested on model immiscible polystyrene/high density polyethylene (PS/HDPE) blends. The influences of mixing time and rotor speed on the mechanical, rheological, and morphology properties of PS/HDPE blends were discussed.

DESCRIPTION OF THE MIXER

General Layout of the Vane Mixer

The self-made vane mixer based on dynamic convergent/divergent flow was schematically represented in Figure 1. The three-dimensional (3D) cutoff view of the mixer was represented in Figure 2. From Figures 1 and 2, we can see that the mixer is mainly composed of one feeding unit and two mixing units. Each unit composed of a stator, a rotor, four vanes, and two baffles. The structure and working principle of the unit were introduced in detail in the previous study.[17,19] The baffles were used to establish a closed space and to control the material flow direction. Two types of baffles were used in this new mixing device to generate circular flow. As shown in Figures 1(a,b) and

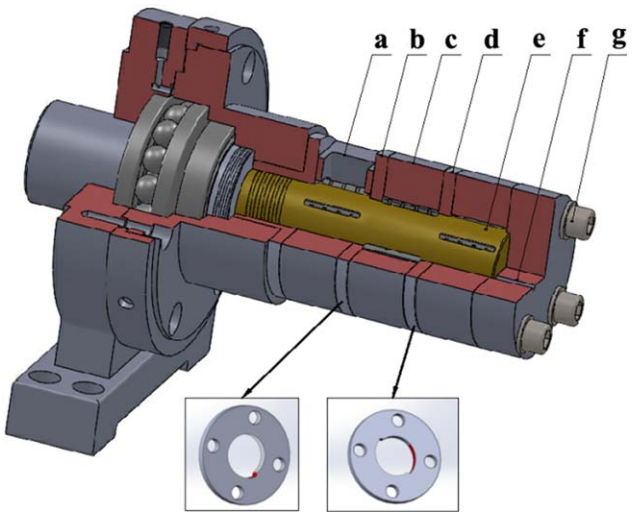

Figure 2. The 3D cutoff view of the vane mixer (a) feeding stator, (b) no-return baffle, (c) mixing stator, (d) circular baffle, (e) rotor, (f) exit channel, and (g) bolt. [Color figure can be viewed in the online issue, which is available at wileyonlinelibrary.com.]

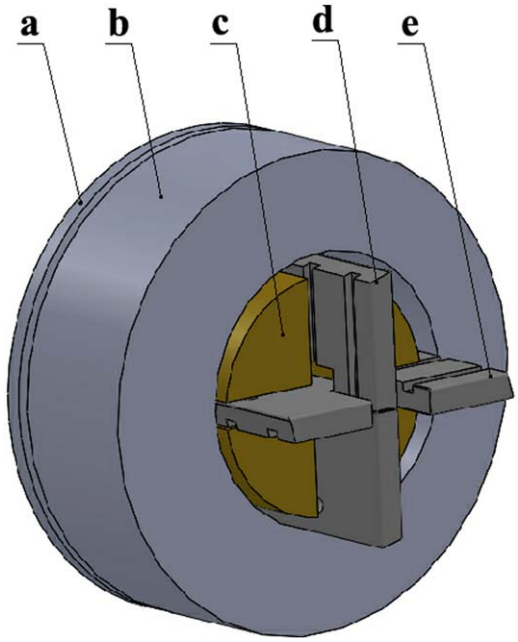

Figure 3. The position relation of the components in a unit (a) baffle, (b) stator, (c) rotor, (d) female vane, and (e) male vane. [Color figure can be viewed in the online issue, which is available at wileyonlinelibrary.com.]

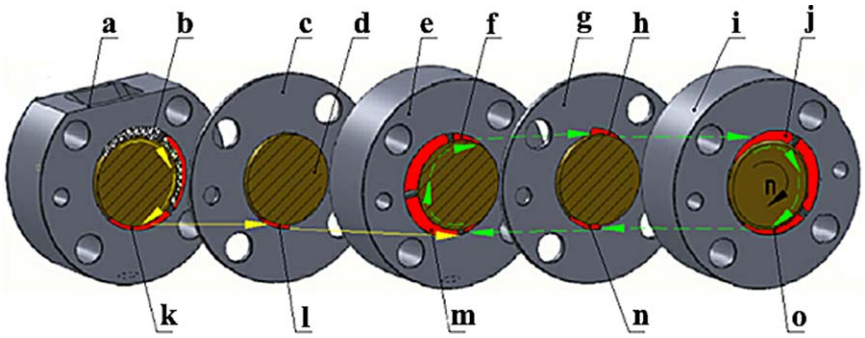

Figure 4. Schematic operation of the vane mixer (a) feeding unit, (b) material, (c) no-return baffle, (d) rotor, (e) mixing unit I, (f) discharging region of mixing unit I, (g) circular baffle, (h) flow gap B, (i) mixing unit II, (j) feeding region of mixing unit II, (k) discharging region of feeding unit, (l) flow gap A, (m) feeding region of mixing unit I, (n) flow gap C, and (o) discharging region of mixing unit II. [Color figure can be viewed in the online issue, which is available at wileyonlinelibrary.com.]

2, there is only one flow gap on the no-return baffle and there are two flow gaps on a circular baffle.

The position relation of the components in a unit was represented in Figure 3. As shown in Figures 1(C-C) and 3, we can see that the rotor is eccentrically installed in the inner hole of the stator. Two male vanes and two female vanes were installed in pairs in the rectangular through hole of the rotor. The pair of vanes makes reciprocating movement in the rectangular through hole of the rotor under the action of the inner surface of the stator as the rotor rotating. This action leads to the periodical changing of the volume constituted by the stator, rotor, two adjacent vanes, and two baffles. The region where the volume decreases as the rotor rotating is called discharge region [Figure 1(C-C)], materials in this space will be forced out through the flow gap on the baffle. On the contrary, the region where the volume increase as the rotor rotating is called feeding region [Figure 1(C-C)], materials will flow into this unit from hopper or the adjacent unit. The eccentric directions of the rotor to the stator of two adjacent units are opposite, that is, one is eccentric to the left and the other is eccentric to the right. In this way, the feeding region and discharging region of mixing unit I are connected with the discharging region and the feeding region of mixing unit II by the flow gaps on the baffle, respectively.

Mixing Procedure

Figure 4 schematically represents the mixing process of the vane mixer. The discharging region of feeding unit connected with the feeding region of mixing unit I through the flow gap on the no-return baffle. However, as there was no flow gap between the feeding region of feeding unit and discharging region of mixing unit I, thus, materials cannot flow back into the feeding unit. The feeding region and the discharging region of mixing unit I are connected with the discharging region and the feeding region of mixing unit II, respectively, through the flow gaps on the circular baffle. Thus, circular flow can be generated between two mixing units as the rotor rotating. The mixing procedure can be divided into three steps as follows:

1. **Feeding**: Materials to be molded were fed into the feeding region of feeding unit and flow into the discharging region where materials were forced out through the flow gap (A) on the no-return baffle and flow into the feeding region of mixing unit I when the rotor rotating. Once all the materials were fed into the mixing unit, no material will flow through flow gap (A).
2. **Mixing**: As the rotor rotating, materials in the feeding region of mixing unit I flow into the discharging region of mixing unit I where materials was forced out through flow gap (B) on the circular baffle and flow into the feeding region of mixing unit II. At the same time, materials in feeding region of mixing unit II flow into the discharging region of mixing unit II, where materials was forced out through flow gap (C) on the circular baffle and flow into the feeding region of mixing unit I as the rotor rotating. Thus, the material undergoes a certain number of mixing cycles, one cycle corresponding to a rotation of the rotor.
3. **Outlet**: When the mixing procedure finished, the blends were forced out from the exit channel [Figure 2(f)]. We also can see from Figure 4 that dynamic extensional deformation can be generated by the dynamic convergent and divergent flow as the geometry of the mixing chamber change periodically. The convergent and divergent flows are expected to contribute significantly to dispersive mixing.

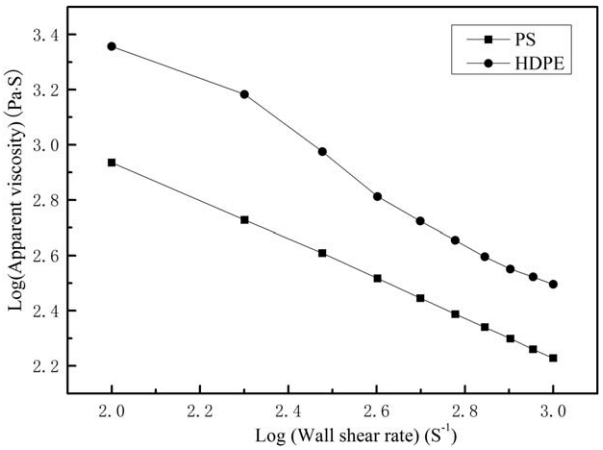

Figure 5. Apparent shear viscosities of (•) HDPE and (■) PS at 190°C.

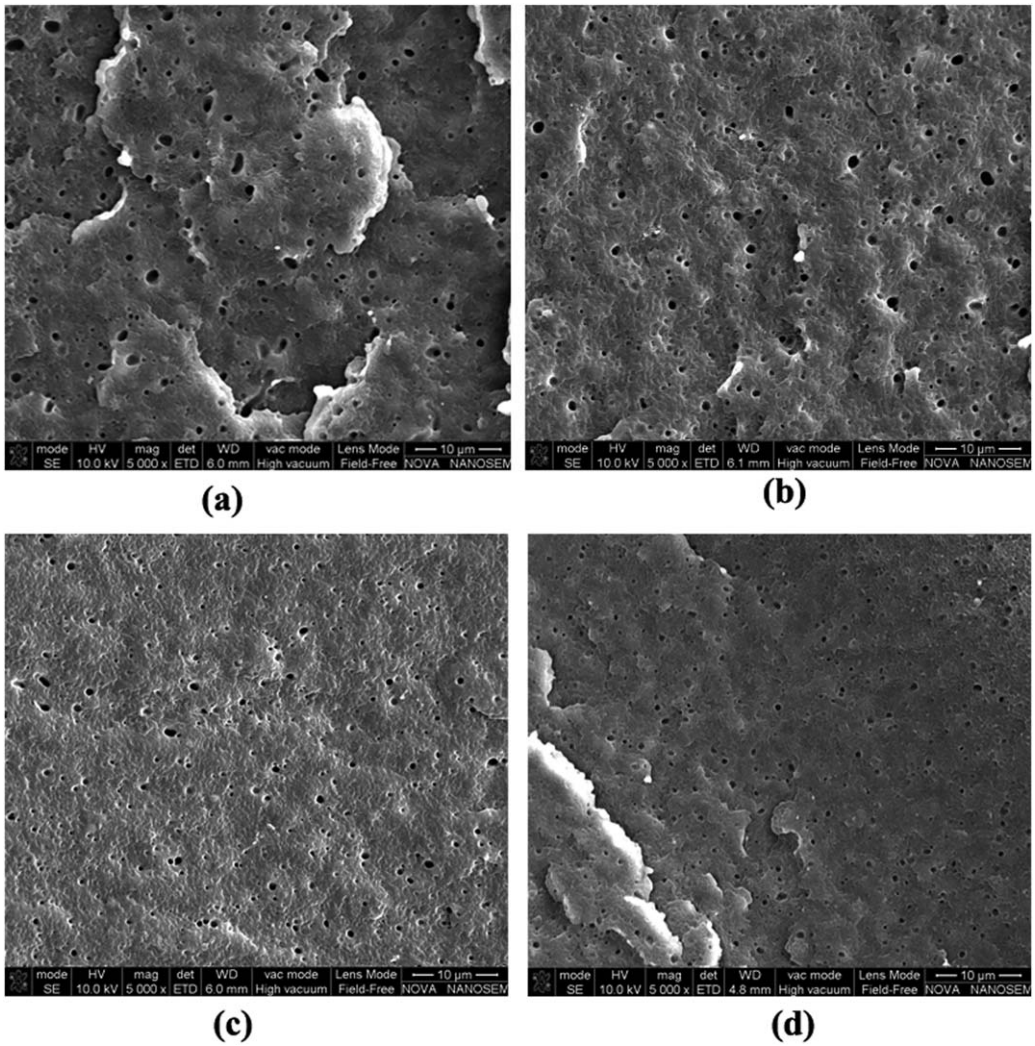

Figure 6. Influence of mixing time on morphology of PS/HDPE blends at 30 rpm (a) 0.5 min, (b) 1 min, (c) 2 min, and (d) 3 min.

EXPERIMENTAL SECTION

Materials

Commercial grades of PS from Hong Kong Petrochemical Company Limited (Trade name: N1841H, Melt flow index 9.5 g/10 min) and HDPE from Petroleum Authority of Thailand (Trade name: HD7000F, Melt flow index 0.045 g/10 min) were used to prepare the binary systems. Viscosities of PE and PS investigated in this study are shown in Figure 5. The shear viscosity was measured by a twin-bore capillary rheometer (Rheologic 5000, Ceast Corporation) with a steel capillary die of 1 mm in diameter and 40 mm in length at 190°C. The ratio of the viscosity of HDPE to that of PS was equal to approximately 1.8 in most range of shear rates.

Preparation of the Blends

Mixtures of PS and PE were melt blended in the self-made vane mixer and a commercialized Brabender mixer at 185°C (Brabender Plasticorder, Model FE-2000). The PS pellets were dried in a vacuum oven for 4 h at 80°C prior to mixing. The components were filled into the mixers in the form of dry blend of pellets. In all cases, the blend composition was 4/96 (PS/HDPE) by weight. To study the influence of the rotor speed and mixing time on the phase morphology, experiments were performed as functions of various mixing time and rotor speed. Mixing time

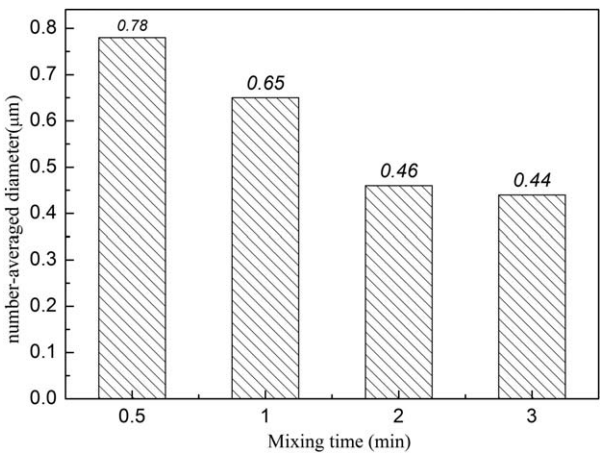

Figure 7. Influence of mixing time on number-averaged diameter at 30 rpm.

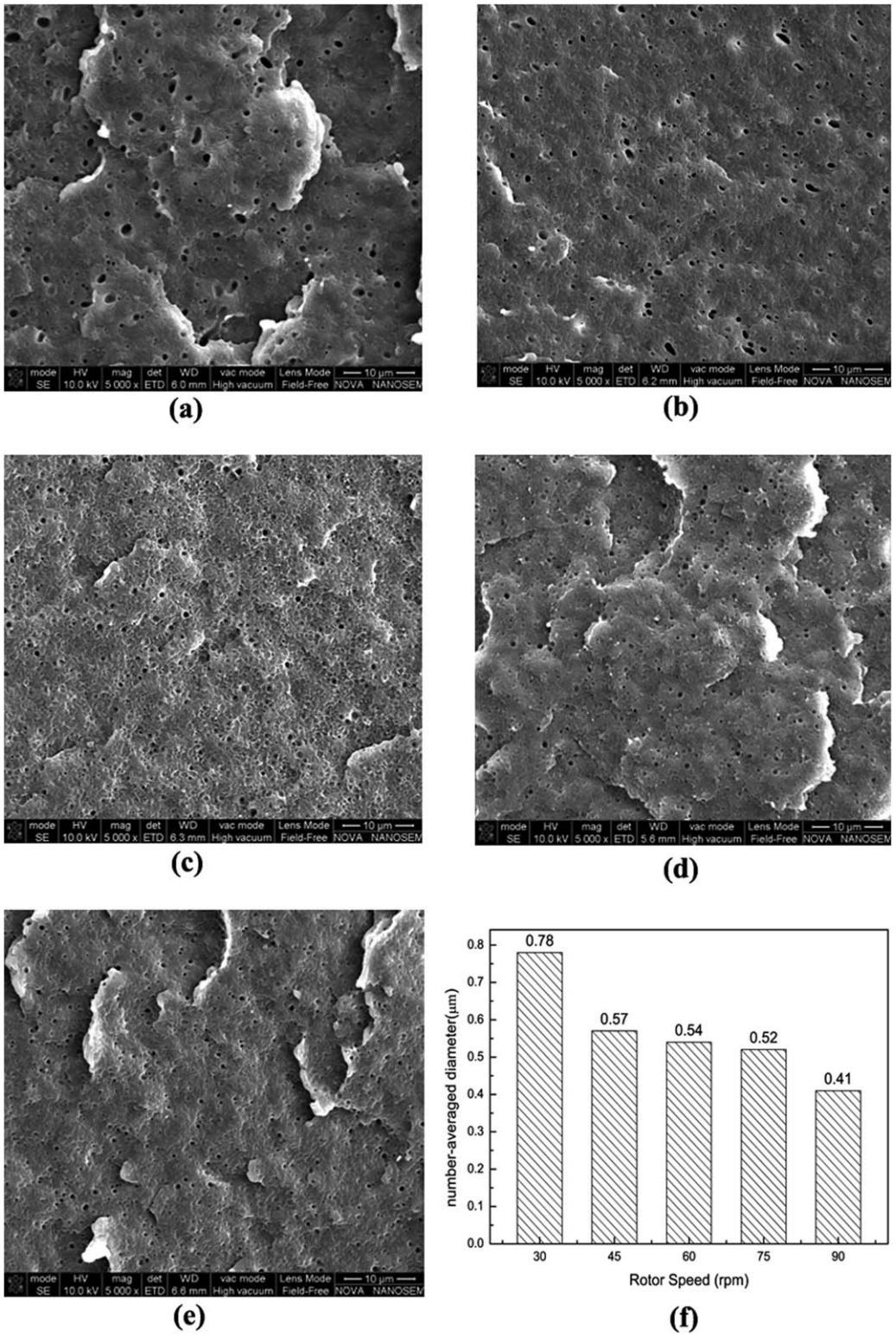

Figure 8. Influence of rotor speed on morphology when mixing time is 0.5 min (a) 30 rpm; (b) 45 rpm; (c) 60 rpm; (d) 75 rpm; (e) 90 rpm; and (f) number-averaged diameter.

varied from 0.5 to 3 min. Rotor speed has been varied from 30 to 90 rpm. In all cases, the material was cooled to room temperature in air at the end of the mixing step.

The new extruder blends were used to characterize the phase morphology and rheological properties. The blends were dried again in a vacuum oven for 4 h at 80°C and then compression

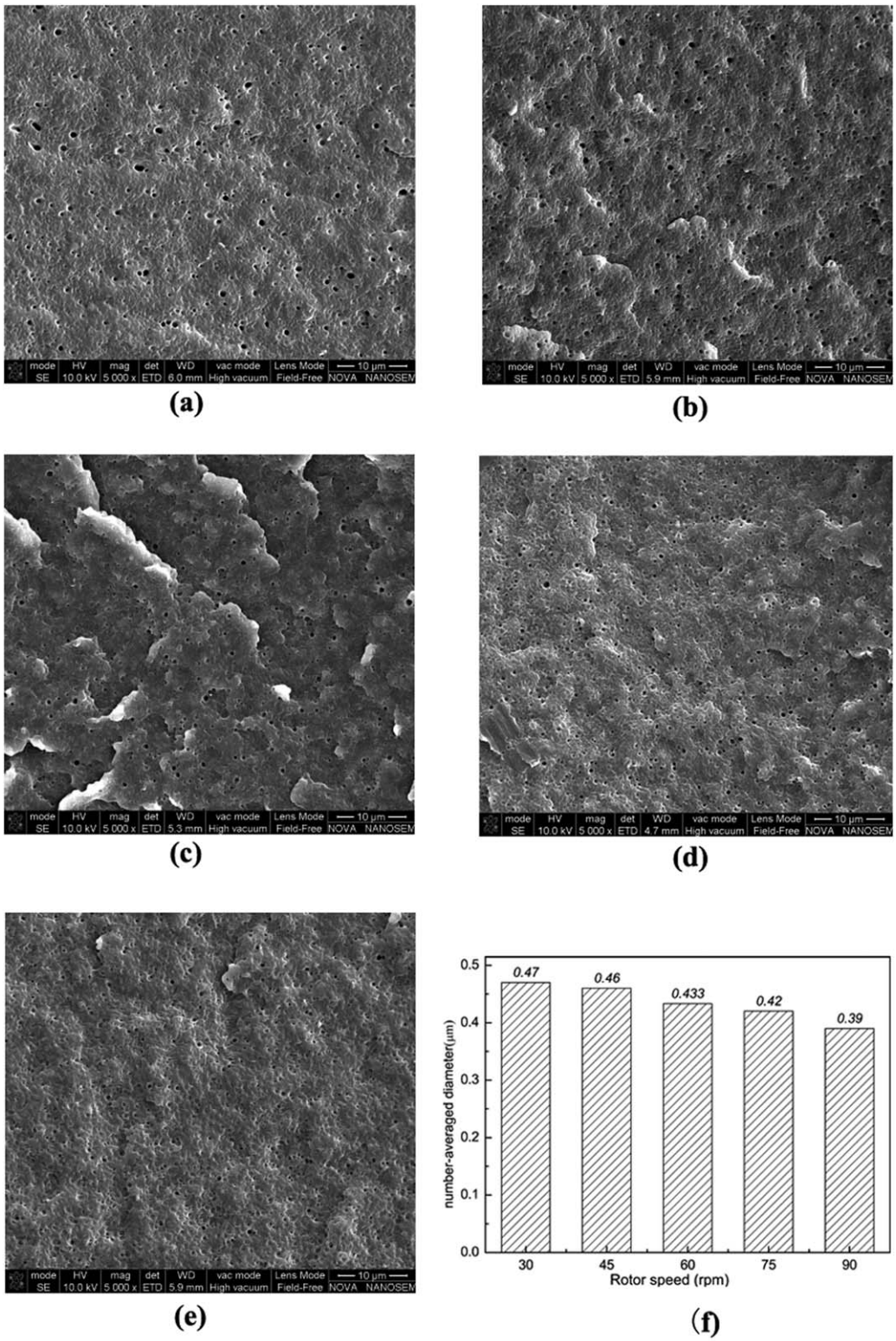

Figure 9. Influence of rotor speed on morphology when mixing time is 2 min (a) 30 rpm; (b) 45 rpm; (c) 60 rpm; (d) 75 rpm; (e) 90 rpm; and (f) number-averaged diameter.

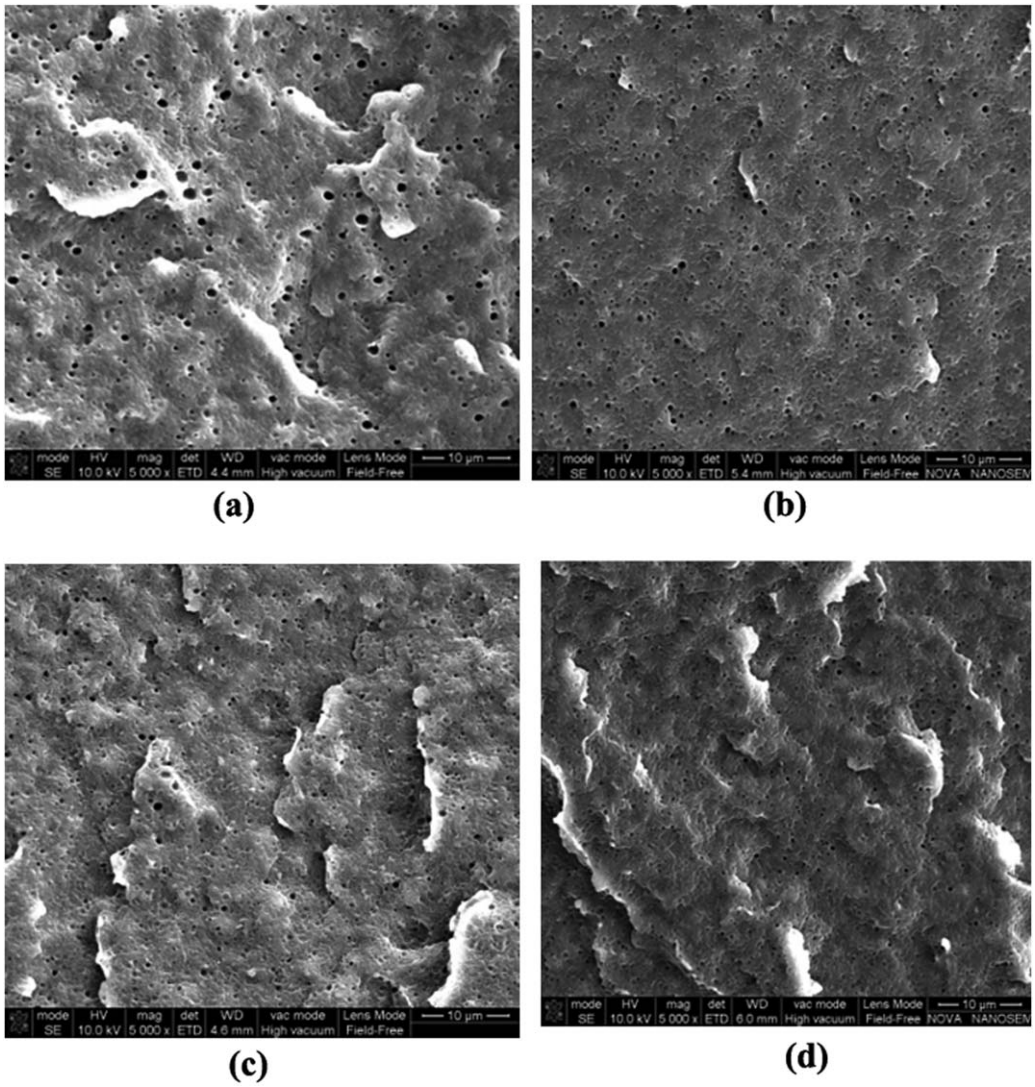

Figure 10. SEM micrographs of PS/HDPE blends produced at 60 rpm in (a) brabender mixer with 1 min mixing time; (b) vane mixer with 1 min mixing time; (c) brabender mixer with 3 min mixing time; and (d) vane mixer with 3 min mixing time.

molded into flat plate with a thickness of 1 mm using a flat plate sulfide machine (QLB-25D/Q). The flat plates were molded at 185°C and a pressure of 10MPa for 15min. Flat plates were cut into dumbbell-shaped tensile test specimens.

Mechanical Testing

A type of Instron 5566 universal testing machine with a tensile speed of 50 mm/min was used, according to the GBT 1447–2005 standard. All tests were performed at ambient temperature (25°C), 50% relative humidity. All the reported values for the tensile strength tests were the average values of five specimens.

Morphology Observation

The samples were fractured in liquid nitrogen. The minor phase (PS) was extracted with cyclohexane to show the dispersed particle size and shape more clearly. The surface of specimens was sputter coated with a thin gold layer to avoid charging during scanning electron microscopy (SEM) imaging. The characterization of the morphology of the prepared samples was performed using SEM (Nova Nano SEM 430, Holland). The accelerating voltage was 10 kV. The dispersed particle size was measured using an automatic image analyzing software (Nano Measurer 1.2.5) developed by department of chemistry, Fudan University, China. The diameter was measured by scanning the micrograph and individually outlining the particles to calculate the dimensions. The droplet diameters d_i was determined assuming a circular shape of the measured area A_i according to eq. (1):

$$di=2\sqrt{\frac{Ai}{\pi}} \tag{1}$$

The number-averaged diameter d_n, was calculated according to eq. (2),

$$dn=\frac{\sum_i nidi}{\sum_i ni} \tag{2}$$

where n_i is the number of particles with diameter d_i. Typically, over 250 particles and several fields of view were analyzed to determine the number average diameter d_n.

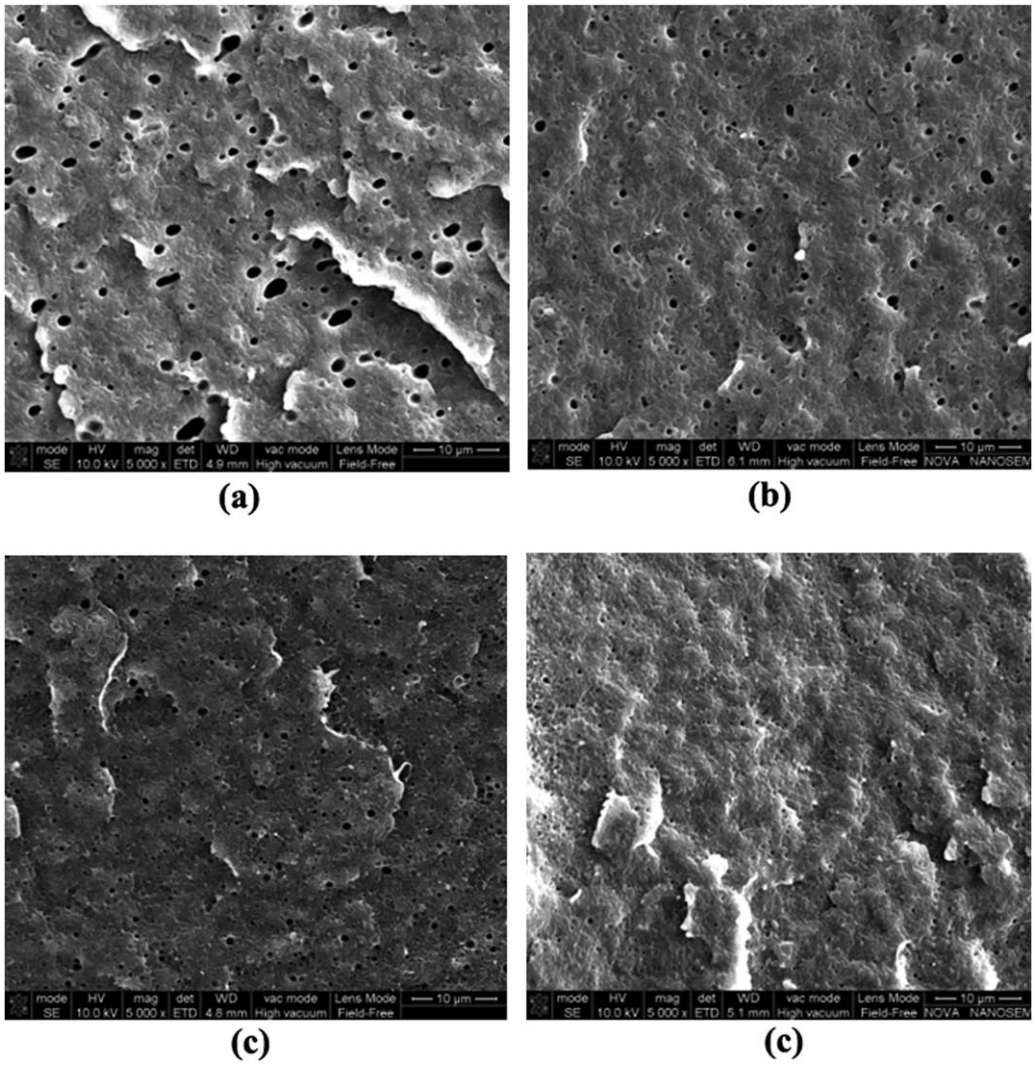

Figure 11. SEM micrographs of PS/HDPE blends produced with 1 min mixing time in (a) Brabender mixer at 30 rpm; (b) vane mixer at 30 rpm; (c) Brabender mixer at 90 rpm; and (d) vane mixer at 90 rpm.

Rheological Characterization

A Ceast twin-bore capillary rheometer (Rheologic 5000, Ceast Corporation) with a capillary diameter of 1 mm and a length-to-diameter ratio of 40 was used to measure the apparent shear viscosities of the blends at the wall shear rates ranging from 100 to 1000 S^{-1}.

RESULTS AND DISCUSSION

Morphology Evolution

Figure 6 shows the SEM images of the PS/HDPE blends prepared in the vane mixer at a constant rotator speed of 30 rpm. The dark areas represent the PS phase and the light areas represent the HDPE phase. It is clear from the photograph that the PS is dispersed as spherical domains in the continuous HDPE matrix. The dispersed phase is reduced to micron-size scale after mixing for only 1 min. Given the fact that the millimeter-sized pellets were initially fed into the mixers, the reduction in phase size is significant and rapid and is similar to the level of phase size reduction in the internal batch mixer.

The influence of mixing time on number-averaged diameter (d_n) was presented in Figure 7. As shown in Figure 7, the number-averaged diameter d_n decreased from 0.78 to 0.65 μm when the mixing time increased from 0.5 to 1 min. The number-averaged diameter d_n decreased from 0.65 to 0.46 μm with the increase of mixing time from 1 to 2 min. However, the number-averaged diameter decreased only 0.02 μm when the mixing time increased from 2 to 3 min. This indicated that the most significant changes in morphology take place within the first 2 min. This was very similar to the previous researches presented by Favis and Li.[20–22]

The influence of rotor speed on structure of PS/HDPE blends when the mixing time was 0.5 min was depicted in Figure 8. As can be seen from Figure 8, the dispersed phase size decreased with the increase of rotor speed at first and then leveled off at higher rotor speed. On one hand, this is mainly because the lower the rotor speed, the lower the strain rate (both shear rate and elongation rate) is. The lower strain rates results in a higher particle size. On the other hand, according to the theory[23,24]

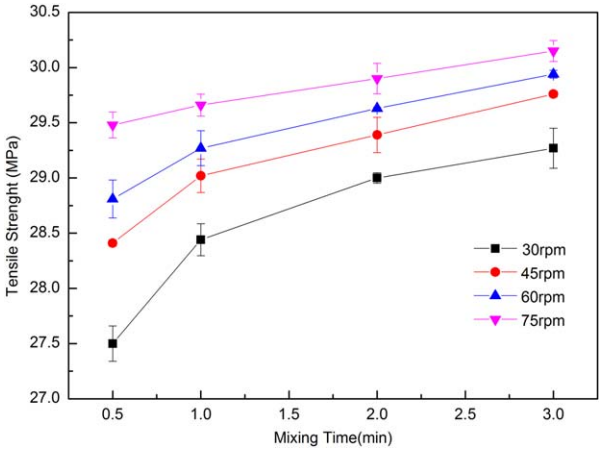

Figure 12. Influence of mixing time on the tensile strength. [Color figure can be viewed in the online issue, which is available at wileyonlinelibrary.com.]

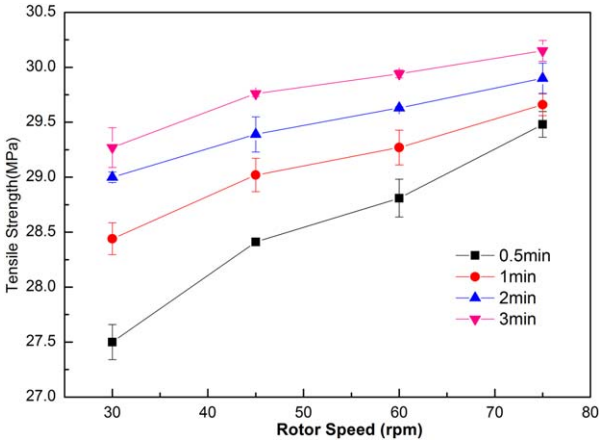

Figure 13. Influence of rotor speed on the tensile strength. [Color figure can be viewed in the online issue, which is available at wileyonlinelibrary.com.]

that the time to break up for the particle is proportional to the diameter of the particle, short mixing time (0.5 min) is not enough to break up the particles at low rotor speed.

The influence of rotor speed on structure of PS/HDPE blends when the mixing time was 2 min was depicted in Figure 9. As can be seen from Figure 9, increasing the rpm from 30 to 90 does not have any major influence on the dispersed phase size. The particle size and particle-size distribution is obviously different from those prepared when the mixing time is 0.5 min. On one hand, although the strain rate is low at low rotor speed, particle can break up to some extent when mixing time is enough. On the other hand, according to Sundararaj's[25] studies, the matrix viscosity decreases and the drop elasticity increase, so that the drop resists the deformation to a greater extent.

Comparison of Morphology Development as a Function of Mixer Type

The morphologies of PS/HDPE blends prepared by a Brabender mixer and a vane mixer at a constant rotator speed are shown in Figure 10. As expected, the particle size is considerably reduced with the increase of mixing time in both type of mixer. The reduction in phase size is significant and rapid in vane mixer than in the Brabender mixer. It is most probably because of the fact that the vane mixer provides the most intensive extensional flow. The majority of flow is shear flow in Brabender mixer. This fact suggests that the vane mixer is more effective than the Brabender mixer.

The morphologies of the PS/HDPE blends prepared using a Brabender mixer and a vane mixer at different rotator speed are shown in Figure 11. The results indicated that the particle size of the blends prepared by vane mixer is much smaller than that of prepared by Brabender mixer at different rotor speed with 1 min mixing time. In the Brabender mixer, the shear rate is considerable to be proportional to the rotor speed. The shear stress/rate is low at slow rotor speed, which caused the higher averaged dispersed particle size. However, in the vane mixer, the convergence is significant and the flow was nearly extensional in the contraction and expansion zones. Thus, finer dispersed particle size and narrower dispersed particle-size distribution were expected at the same rotor speed and mixing time.

Tensile Strength

Figures 12 and 13 show the tensile strength of the PS/HDPE composites as functions of mixing time and rotor speed, respectively. As can be seen from Figures 12 and 13, the tensile strength increased quickly at first and then leveled off with the increase of mixing time or rotor speed. The variation in tensile strength is not substantial. The increase of tensile strength can be ascribed to the finer dispersion of PS phase in HDPE. On one hand, finer dispersion of PS phase in HDPE enhanced interfacial adhesion of the blends, making stress transfer more efficient between phases during fracture. On the other hand, finer dispersion of PS phase in HDPE results in lower resultant stress concentration, which improved the tensile properties of the blends.

Rheological Characterization

Figure 14 shows the influence of mixing time on blends apparent viscosity when rotor speed is 90 rpm. Figure 15 shows the

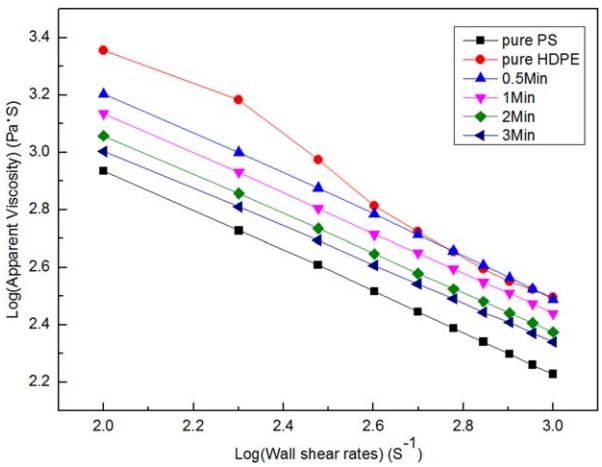

Figure 14. Influence of mixing time on apparent viscosity of blends. [Color figure can be viewed in the online issue, which is available at wileyonlinelibrary.com.]

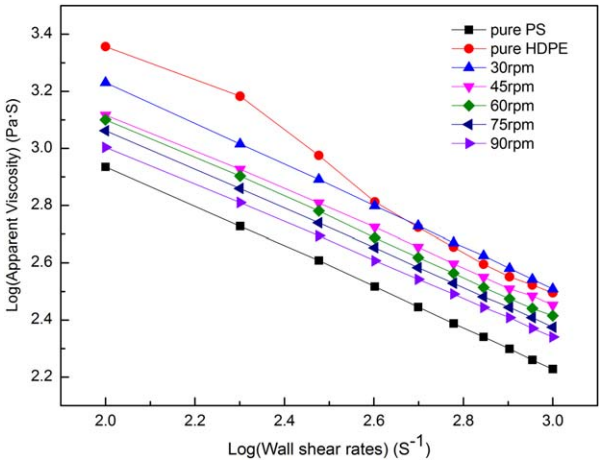

Figure 15. Influence of rotor speed on blends apparent viscosity. [Color figure can be viewed in the online issue, which is available at wileyonlinelibrary.com.]

influence of rotor speeds on blends apparent viscosity with 3 min mixing time. As can be seen from Figures 14 and 15, the apparent shear viscosity curves of the blends are between those of the pure components. The data demonstrated a decrease in the viscosity of the blends when 4 wt % PS was incorporated in the blends. As the viscosity of PS phase is lower, a viscosity drop of the blends is understandable. It is commonly accepted that the rheological properties of a two-phase system depend on not only the rheological behavior of the components but also the size and size distribution and shape of the discrete droplets dispersed in a continuous matrix phase. As discussed in the earlier paragraph, the particles size decreased with the increase of mixing time at given rotor speed or decreased with the increasing of rotor speed at constant mixing time. On one hand, the decrease of apparent shear viscosity can be ascribed to the large droplets in the blends are easy to coalesce, which cause an increase in the apparent viscosity to occur at this concentration of PS. On the other hand, finer PS dispersion in the HDPE matrix acts as plasticizer which reduced the flow resistance of the HDPE phase, which caused the decrease of the blends apparent viscosity.

CONCLUSIONS

A new type of mixer was successfully designed and built, and the performance of the mixer was evaluated. The mixer was designed to utilize dynamic extensional deformation generated by the periodically changed convergent/divergent geometry. Experiment results show that the mixer developed shows both excellent dispersive and distributive mixing efficiency. In addition, the mixer has mixing chamber of very simple geometry, the cleaning is very easy, and the material lost is very small.

ACKNOWLEDGMENTS

The financial support from the National Science and Technology Pillar Program during the Twelve Five-Year Plan period (2011BAE15b01), the National Natural Science Funds (51403068) and the Fundamental Research funds for the Central Universities of China 2013ZZ0015, 2013ZM0014 are gratefully acknowledged.

REFERENCES

1. Rauwendaal, C. *Plast. Addit. Compd.* **2008**, *10*, 32.
2. Rauwendaal, C. *Plast. Addit. Compd.* **1999**, *1*, 21.
3. Delaby, I.; Ernst, B.; Muller, R. *J. Macromol. Sci. Phys.* **1996**, *35*, 547.
4. Delaby, I.; Ernst, B.; Muller, R. *Rheol. Acta.* **1995**, *34*, 525.
5. Milliken, W. J.; Leal, L. G. *J. Nonnewtonian Fluid Mech.* **1991**, *40*, 355.
6. Meller, M.; Luciani, A.; Månson, J. A. *Int. Polym. Process.* **1999**, *14*, 221.
7. Meller, M.; Luciani, A.; Mårnson, J. A. *Polym. Eng. Sci.* **2002**, *42*, 634.
8. Luciani, A.; Utracki, L. A. *Int. Polym. Process.* **1996**, *11*, 299.
9. Son, Y. *J. Appl. Polym. Sci.* **2009**, *112*, 609.
10. Mackley, M. R.; Marshall, R. T. J.; Smeulders, J. B. A. F. *J. Rheol.* **1995**, *39*, 1293.
11. Bouquey, M.; Loux, C.; Muller, R.; Bouchet, G. *J. Appl. Polym. Sci.* **2011**, *119*, 482.
12. Rauwendaal, C.; Osswald, T.; Gramann, P. *Int. Polym. Process.* **1999**, *14*, 28.
13. Rauwendaal, C. *Plast. Addit. Compd.* **2008**, *10*, 32.
14. Rauwendaal, C. *Plast. Technol.* **2012**, *58*, 30.
15. Terrisse, J.; Muller, R.; Bouquey, M. WO2008142234-A1, **2007**.
16. Qu, J. P. *Eur. Pat.* 2113355-A1, **2013**.
17. Qu, J. P.; Zhang, G. Z.; Chen, H. Z. *Polym. Eng. Sci.* **2012**, *52*, 2147.
18. Zheng-Huan, W.; Yong-Qin, Z.; Gui-Zheng, Z. *J. Appl. Polym. Sci.* **2013**, *130*, 2328.
19. Rondin, J.; Bouquey, M.; Muller, R. *Polym. Eng. Sci.* **2014**, *54*, 1444.
20. Scott, C. E.; Macosko, C. W. *Polym. Bull.* **1991**, *26*, 341.
21. Li, H. X.; Hu, G.-H. *J. Polym. Sci. B Polym. Phys.* **2001**, *39*, 601.
22. Oommen, Z.; Zachariah, S. R.; Thomas, S. *J. Polym. Sci. B Polym. Phys.* **2004**, *43*, 1025.
23. Elemans, P. H. M.; Janssen, J. M. H.; Meijer, H. E. H. *J. Rheol.* **1990**, *34*, 1311.
24. Palmer, G.; Demarquette, N. R. *Polymer* **2003**, *44*, 3045.
25. Sundararaj, U.; Macosko, C. W.; Rolando, R. J.; Chan, H. T. *Polym. Eng. Sci.* **1992**, *32*, 1814.